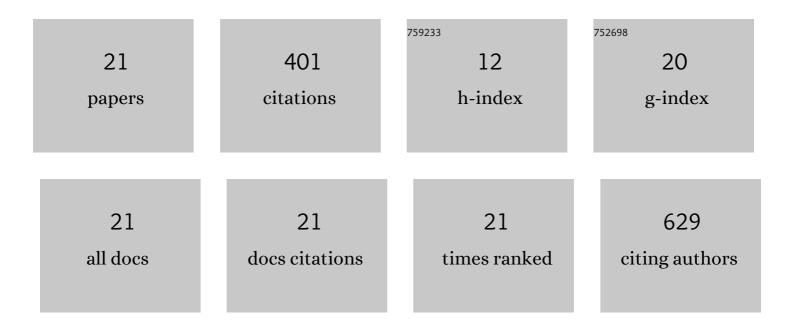
Teruyoshi Uetani

List of Publications by Year in descending order

Source: https://exaly.com/author-pdf/3464477/publications.pdf Version: 2024-02-01



#	Article	IF	CITATIONS
1	Coronary artery stenosis-related perfusion ratio using dynamic computed tomography myocardial perfusion imaging: a pilot for identification of hemodynamically significant coronary artery disease. Cardiovascular Intervention and Therapeutics, 2020, 35, 327-335.	2.3	6
2	Combined assessment of subtended myocardial volume and myocardial blood flow for diagnosis of obstructive coronary artery disease using cardiac computed tomography: A feasibility study. Journal of Cardiology, 2020, 76, 259-265.	1.9	2
3	Clinical application of four-dimensional noise reduction filtering with a similarity algorithm in dynamic myocardial computed tomography perfusion imaging. International Journal of Cardiovascular Imaging, 2020, 36, 1781-1789.	1.5	10
4	Diagnostic accuracy of stress myocardial computed tomography perfusion imaging to detect myocardial ischemia: a comparison with coronary flow velocity reserve derived from transthoracic Doppler echocardiography. Journal of Cardiology, 2020, 76, 251-258.	1.9	1
5	Characteristics of the left ventricular three-dimensional maximum principal strain using cardiac computed tomography: reference values from subjects with normal cardiac function. European Radiology, 2020, 30, 6109-6117.	4.5	8
6	Evaluation of Significant Coronary Artery Disease Based on CT Fractional Flow Reserve and Plaque Characteristics Using Random Forest Analysis in Machine Learning. Academic Radiology, 2020, 27, 1700-1708.	2.5	12
7	Deletion of interleukin-18 attenuates abdominal aortic aneurysm formation. Atherosclerosis, 2019, 289, 14-20.	0.8	23
8	Impact of the sampling rate of dynamic myocardial computed tomography perfusion on the quantitative assessment of myocardial blood flow. Clinical Imaging, 2019, 56, 93-101.	1.5	14
9	Impact of Knowledge-Based Iterative Model Reconstruction on Image Quality and Hemodynamic Parameters in Dynamic Myocardial Computed Tomography Perfusion Using Low-Tube-Voltage Scan. Journal of Computer Assisted Tomography, 2019, 43, 811-816.	0.9	8
10	Incremental diagnostic value of whole-heart dynamic computed tomography perfusion imaging for detecting obstructive coronary artery disease. Journal of Cardiology, 2019, 73, 425-431.	1.9	13
11	Late iodine enhancement computed tomography with image subtraction for assessment of myocardial infarction. European Radiology, 2018, 28, 1285-1292.	4.5	12
12	Biochemical and histological evidence of deteriorated bioprosthetic valve leaflets: the accumulation of fibrinogen and plasminogen. Biology Open, 2018, 7, .	1.2	32
13	Intravascular Ultrasound-Derived Virtual Fractional Flow Reserve for the Assessment of Myocardial Ischemia. Circulation Journal, 2018, 82, 815-823.	1.6	24
14	Peak enhancement ratio of myocardium to aorta for identification of myocardial ischemia using dynamic myocardial computed tomography perfusion imaging. Journal of Cardiology, 2017, 70, 565-570.	1.9	2
15	Estimation of myocardial flow reserve utilizing an ultrafast cardiac SPECT: Comparison with coronary angiography, fractional flow reserve, and the SYNTAX score. International Journal of Cardiology, 2017, 244, 347-353.	1.7	45
16	Intracoronary Optical Coherence Tomography-Derived Virtual Fractional Flow Reserve for the Assessment of Coronary Artery Disease. American Journal of Cardiology, 2017, 120, 1772-1779.	1.6	43
17	Perivascular Adipose Tissue Angiotensin II Type 1 Receptor Promotes Vascular Inflammation and Aneurysm Formation. Hypertension, 2017, 70, 780-789.	2.7	53
18	Three-dimensional maximum principal strain using cardiac computed tomography for identification of myocardial infarction. European Radiology, 2017, 27, 1667-1675.	4.5	26

#	Article	IF	CITATIONS
19	Correlation Between Quantitative Angiography–Derived Translesional Pressure and Fractional Flow Reserve. American Journal of Cardiology, 2016, 118, 1158-1163.	1.6	9
20	Differentiation of myocardial ischemia and infarction assessed by dynamic computed tomography perfusion imaging and comparison with cardiac magnetic resonance and single-photon emission computed tomography. European Radiology, 2016, 26, 3790-3801.	4.5	41
21	Insufficiency of Pro-heparin-binding Epidermal Growth Factor-like Growth Factor Shedding Enhances Hypoxic Cell Death in H9c2 Cardiomyoblasts via the Activation of Caspase-3 and c-Jun N-terminal Kinase. Journal of Biological Chemistry, 2009, 284, 12399-12409.	3.4	17